Microfluid Nanofluid (2012) 13:75–82
DOI 10.1007/s10404-012-0942-6

RESEARCH PAPER

# Self-encapsulated hollow microstructures formed by electric field-assisted capillarity

**H. Chen · W. Yu · S. Cargill · M. K. Patel · C. Bailey · C. Tonry · M. P. Y. Desmulliez**

Received: 18 October 2011 / Accepted: 16 January 2012 / Published online: 2 February 2012


**Abstract** Hollow microstructures serve many useful applications in the fields of microsystems, chemistry, photonics, biology and others. Current fabrication methods of artificial hollow microstructures require multiple fabrication steps and expensive manufacturing tools. The paper reports a unique one-step fabrication process for the growth of hollow polymeric microstructures based on electric field-assisted capillary action. This method demonstrates the manufacturing of self-encapsulated microstructures such as hollow microchannels and microcapsules of around 100-μm height from an initial polymer thickness of 22 μm. Microstructure caps of several microns thickness have been shown to keep their shape under bending or delamination from the substrate. The inner surface of hollow microstructures is shown to be smooth, which is difficult to achieve with current methods. More complicated structures, such as a microcapsule array connected with hollow microchannels, have also been manufactured with this method. Numerical simulation of the resist growth process using COMSOL Multiphysics finite element analysis software has resulted in good agreement between simulated and experimental results on the overall shape of the resulting structures. These results are very positive and demonstrate the speed, versatility and cost-effectiveness of the method.

**Keywords** Microfluidics · Electrohydrodynamic · Instabilities · Capillary · Hollow microstucture · High-aspect ratio microfabrication

H. Chen · W. Yu (✉)
State Key Laboratory of Applied Optics, Changchun Institute of Optics, Fine Mechanics and Physics, Chinese Academy of Sciences, 3888 Dongnanhu Road, Changchun, Jilin, People's Republic of China
e-mail: yuwx@ciomp.ac.cn

H. Chen
Graduate School of the Chinese Academy of Science, Beijing 10039, People's Republic of China

S. Cargill · M. P. Y. Desmulliez
Microsystems Engineering Center (MISEC), School of Engineering and Physical Sciences, Heriot-Watt University, Earl Mountbatten Building, Edinburgh EH14 4AS, UK
e-mail: m.desmulliez@hw.ac.uk

M. K. Patel · C. Bailey · C. Tonry
School of Computing and Mathematical Sciences, University of Greenwich, Old Royal Naval College, Park Row, London SE10 9LS, UK

## 1 Introduction

Hollow microstructures have found a wide range of applications in fields as diverse as photonics, microfluidics, microelectronics, chemistry and biology. In chemistry or biotechnology, hollow microchannels have been used as the basic elements of microfluidic systems encompassing thousands of integrated micromechanical valves and pumps to achieve high-throughput processes (Unger et al. 2000; Thorsen et al. 2002; Melin and Quake 2007). In biomedical applications, hollow structures have been used extensively as receptacles for drugs and DNA, whose encapsulation and release are achieved with the shell of such structures (Cai et al. 2007; Zhu et al. 2005; Sokolova et al. 2006). Two manufacturing techniques are traditionally employed to manufacture hollow structures. The first approach (chemical etching), borrowed from the microelectronics industry, uses a sacrificial layer removed at the end of the process to form the cavity within the hollow microstructure (Barber et al. 2005; Guijt et al. 2001;

Peeni et al. 2006). The second approach (membrane-assisted microtransfer molding method) uses a bonding process together with a membrane to cap microchannels fabricated by soft lithography (Unger et al. 2000; Thorsen et al. 2002; Xia and Whitesides 1998; Choi et al. 2011). The chemical etching based bottom-up manufacturing technique relies on the state-of-the-art control of chemical reactions at the molecular level to form core–shell structures (Lou et al. 2008). Although it has been elegantly demonstrated that 3-D microstructures can be fabricated by employing the membrane-assisted microtransfer molding method, it is not possible for soft lithography to replicate fully encapsulated or sealed hollow microstructures in a single step (LaFratta et al. 2006). Both these methods have their advantages and disadvantages. The main disadvantage of the chemical etching method lies in the complexity of the fabrication of hollow structures at the wafer-level scale, making it very difficult to integrate with current semiconductor manufacturing cycles. Similarly, the membrane-assisted microtransfer molding method involves multiple steps, which make the method time consuming and expensive.

The new approach driven by an electric field and capillary forces, termed electric field-assisted capillarity (EFAC), demonstrates a simple yet cost-effective and faster method to fabricate hollow polymeric microstructures. The presence of an electric field close to a liquid polymer surface has been demonstrated to induce instabilities of the polymer–air interface and thereby control the morphology of the surface (Schaffer et al. 2000, 2001; Salac et al. 2004; Lin et al. 2002; Marariu et al. 2002; Atta et al. 2011). The resulting electrostatic induced deformation method has been developed to realize the micro- and nanofabrication of features in polymeric materials (Schaffer et al. 2000, 2001; Salac et al. 2004; Lin et al. 2002; Marariu et al. 2002; Wu and Russel 2009). A microfabrication method based on capillary action only, called capillary force lithography, has also been demonstrated in polymers (Suh et al. 2001; Suh and Lee 2002; Bruinink et al. 2006).

This work combines aspects of these two techniques (electric field and capillary forces) for the one-step fabrication of self-encapsulated hollow polymeric microstructures in polymers. The schematic of the fabrication process used to demonstrate the proposed method is illustrated in Fig. 1 and explained in the following section.

## 2 Materials and method

A schematic of the manufacturing process is shown in Fig. 1: (a) the experimental setup consists of a top patterned electrode (the master) and a bottom electrode. Liquid polymer is coated onto the bottom electrode. A controlled air gap exists between the top electrode and the polymer surface. A hotplate is used to heat the polymer just above the glass transition temperature, although UV curable polymers can also be used to alleviate the use of the hotplate. (b) The electrostatic field, present between the two electrodes, destabilizes the thin viscous polymer film and induces the microstructure growth upward toward the top electrode. (c) Once the polymer fully touches the top electrode (see Fig. 1b), capillary forces drive the liquid polymer into the microcavity such that the whole surface of the top electrode is coated by the polymer. (d) The polymer is then either heated to solidify the hollow structure or UV cured, and then released from the top electrode.

To demonstrate this one-step manufacturing process, a patterned nickel master was fabricated using the UV-LIGA process. A glass wafer substrate was deposited with a multilayered Ti/Cu/Ti metal thin film by an e-beam evaporator to render its surface electrically conductive. A thin layer of polydimethylsiloxane (PDMS, Dow Corning, Sylgard 184) polymer solution was spin coated onto the substrate. Properties of the PDMS material are given in Table 1. Spacers were patterned for the experiment to provide a fixed gap between the top electrode and the polymer film. Alternatively, a high precision placement machine can be employed to control the distance between the nickel master and the liquid polymer. The fabrication process is quite simple and described as follows. Firstly, an AC electric field of 1 kV peak-to-peak output voltage with a frequency of 50 Hz was applied to the pre-cured PDMS for 1 h to induce the destabilization of the film and the redistribution of the PDMS monomers under the drive of spatially modulated electrostatic pressure. The frequency has been shown not to be a critical parameter of the manufacturing process. A hotplate was then used to heat the PDMS for 30 min at 150°C to polymerize the PDMS monomers and thus solidify the microstructure formed. After 30 min of curing and another hour of cooling down to room temperature, the PDMS was carefully separated manually from the master electrode for further characterization. Steps can be taken to reduce the overall time of the process.

## 3 Description of the electric field-assisted capillary process

The formation of hollow structures by using electric field-assisted capillary action can be explained as follows. In the first stage of the process, the strong spatially modulated electric field ($\sim 1 \times 10^7$ $\mathrm{Vm}^{-1}$) destabilizes the polymer–air interface and therefore drives the flow of the polymer from regions of low to high electric field (Schaffer et al. 2000, 2001; Wu and Russel 2009). As the polymer grows

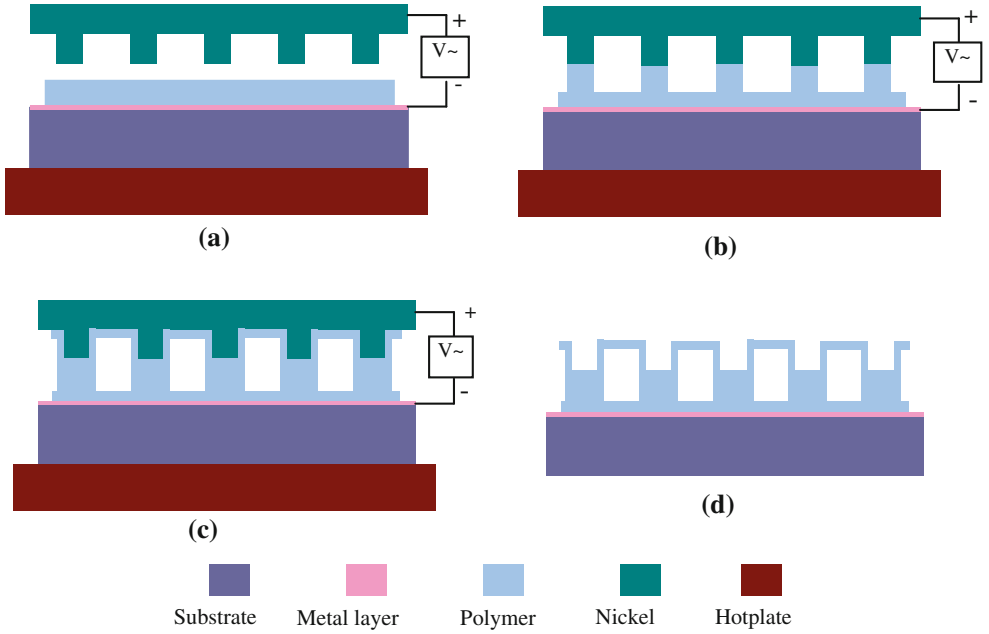


**Fig. 1** Schematic of the hollow microstructure manufacturing process

**Table 1** Typical properties of PDMS (Sylgard 184, Dow Corning): mix ratio is by weight or volume of base/curing agent

| Dynamic viscosity (centipoise) | Specific gravity (25°C) | Dielectric constant (100 Hz) | Dielectric constant (100 kHz) | Mix ratio |
|---|---|---|---|---|
| 4,575 | 1.03 | 2.72 | 2.68 | 10:1 |

Source of the data: data sheet of Dow Corning (http://www1.dowcorning.com/DataFiles/090007c88020bcca.pdf)

in the regions of high electric field induced by the patterns of the master electrode, there comes a time when the polymer touches the bottom surface of the protrusions of the nickel master, where capillary forces become dominant. As the movement of polymer continues due to the action of the electric field, the polymer flows into the microcavity under a capillary force. The adhesive force of PDMS polymer onto nickel is larger than its cohesive force as the polymer, in its liquid form, has a very low surface tension ($\sim$20 mN/m) and a high degree of flowability. As a result, the polymer flows upward into the microcavity along the sidewalls of the patterns of the master electrode. If the polymer film is thick enough, such that enough material can be driven upward, and provided that the electrostatic and capillary forces keep driving the polymer into the microcavity, the polymer will not only cover the whole sidewalls but also the bottom of the cavity. In other words, the whole surface of the nickel master will be covered by the polymer resulting in the formation of a very thin membrane acting as a cap for the hollow microstructure.

Further experiments are needed to define the critical initial film thickness to allow the enclosed cap of the hollow microstructure to form. The duration of each stage of the process (film instability, capillary filling, encapsulation) is also difficult to measure due to the lack of effective in situ monitoring equipment. The duration allowed for the whole process, 1 hour, guarantees the full encapsulation of the channels, although it is likely that this duration can be considerably shortened. Future work should include the development of an effective method for the real-time in situ monitoring of the whole process.

The presented manufacturing method differs in many aspects from capillary force lithography. In the latter, either a flexible mold or a flexible substrate is necessary to ensure the intimate contact between the mold and the substrate to facilitate capillary effects. However, in the proposed method, both mold and substrate are hard. The intimate contact between the mold and the polymer is achieved by a flowing polymer induced by the electric field as shown in Fig. 1b. Furthermore, capillary force lithography requires the mold to be in contact with the polymer coated on the substrate during the entire fabrication process. Here, there is an air gap and the mold does not come into contact with the polymer initially. This contact-free method allows one to manufacture high-aspect-ratio hollow structures by using a relatively low-aspect-ratio and therefore cheaper master.

The balance of forces applied on the polymer is also different from the one found in the traditional capillary

action. As shown in Fig. 2a, the capillary rise of the polymer into the cavity causes the increase of the trapped air pressure, $P_a$. When the air pressure equals the Laplace pressure, $P_L$, the capillary rise stops and a meniscus is created. However, in the case of the formation of hollow microstructure by electrostatic pressure, when the grown polymer touches the mold, the volume of the trapped air will not change anymore and thus the air pressure is always $P_0$ as shown in Fig. 2b. Therefore, once the polymer liquid flows into the cavity under the capillary action, the polymer flow will not stop until the whole inner surface of the microcavity is covered by the polymer liquid. By controlling the initial thickness of the polymer deposited, it is possible to guarantee that the microcavity created by such a method is never completely filled. Finally, the flow of the polymer solution inside the microcavity is also eased by the reduction of the surface tension of the polymer liquid due to the surface charges at the solid–liquid interface as defined by the Lippman equation (Lippmann 1875; Squires 2005),

$$\gamma_{sl}(V) = \gamma_{sl0} - \frac{1}{2}cV^2 \quad (1)$$

The resulting contact angle is modified as

$$\cos\theta_E = \cos\theta + \frac{cV^2}{2\gamma} \quad (2)$$

Where $\gamma_{sl0}$ refers to the surface tension without charge, $V$ is the electric potential between the two electrodes, $c$ is the capacitance of the structure, $\gamma$ is the surface tension of liquid–gas interface, and $\theta$ and $\theta_E$ refer to the contact angle without and with charge, respectively. Equation 2 shows that the contact angle decreases with the voltage, facilitating therefore capillarity. Previously studied capillary force lithography is limited by the size of the cavity (Suh et al. 2001; Suh and Lee 2002; Bruinink et al. 2006): the smaller the size the more favorable is the capillary rise. As a result, it is relatively difficult for capillary force lithography to work at the micron scale. However, in the proposed process, hollow microstructures as high as 350 μm have been fabricated successfully as described later in this article.

## 4 Numerical simulation

A simple model was developed in COMSOL MULTIPHYSICS (Version 4.0, COMSOL group) to look at the evolution of the structure due to the electrostatic force and surface tension at the interface of the liquid polymer. For this model, the liquid is considered to be incompressible, and the incompressible Navier–Stokes equations are introduced to describe the liquid. The phase field method for two phase-flow module and electrostatics module were also employed. In the model, a segment of an array of semicircular electrodes is considered. As the model is 2D and nonaxisymmetric, it is assumed to be an infinite plane in the third dimension. The symmetry of the problem was also exploited and only half the electrode was modeled to speed up the simulations.

The geometry and mesh of the model are presented in Fig 3. The DC voltage applied between the bottom (boundary 2) and the top electrode (boundaries 5, 12 and 14) is 250 V. The boundary conditions for the fluid flow are: (a) no slip at boundary 2; (b) symmetry boundary on boundaries 9, 10 and 11; (c) slip wall at boundaries 1, 3 and 5; and (d) a wetted wall on boundaries 12 and 14; the contact angle of the liquid polymer is assumed to be 20°. The properties of the polymer liquid used in simulation are presented in Table 2. The viscosity is about 1/5th of the real viscosity. This is a numerical trick that allows faster turnaround time for the simulations by way of fewer time steps. For simplicity, a DC electric field has been used rather than the AC field used in the experiments.

The electrostatic forces are assumed to be applied at the fluid–air interface, i.e., any free charges are gathered at the interface due to the electrostatic force pulling them toward the top of the fluid. The electric field is solved by assuming

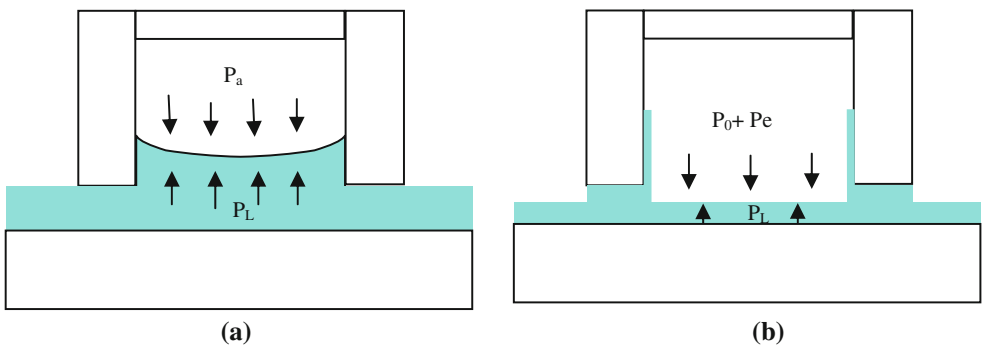


**Fig. 2** Schematic illustration of the capillary action in capillary force lithography (**a**) and in the formation of the hollow microstructure by electric field-assisted capillary action (**b**). $P_L$ and $P_e$ are the Laplace pressure and the electrostatic pressure, respectively

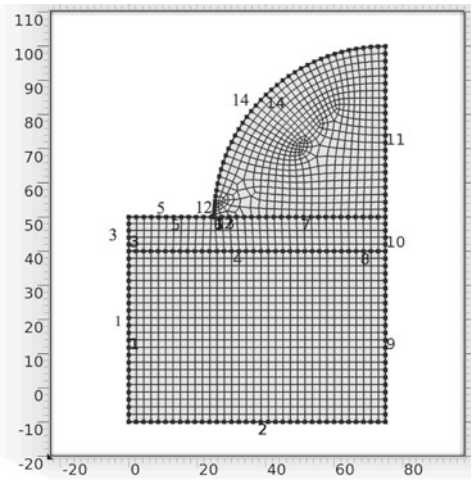


**Fig. 3** Geometry, boundary condition and mesh. Dimensions in μm

| No | Boundary Conditions (Flow/E-field) |
|---|---|
| 1 | Slip wall/Symmetry for V |
| 2 | No slip Wall/ 0V |
| 3 | Slip wall/Symmetry for V |
| 5 | Slip Wall/250V |
| 6 | Wetted Wall 20° |
| 9 | Symmetry |
| 10 | Symmetry |
| 11 | Symmetry |
| 12 | 250V |
| 13 | Wetted Wall 20° |
| 14 | Wetted Wall 20°/250V |

**Table 2** Use of material properties in the numerical simulations

| Simulation dynamic viscosity (centipoise) | Specific gravity (25°C) | Dielectric constant (100 Hz) | Surface tension (mN/m) |
|---|---|---|---|
| 1,000 | 1.03 | 2.72 | 20 |

that there are no free charges in the rest of the fluid. Both assumptions give rise to the equations governing the force on the interface; firstly the electric field is solved using the Laplace's equation for the voltage (Eq. 3):

$$\nabla \varepsilon \nabla V = 0 \tag{3}$$

The spatial derivative of the voltage is used to prescribe the electric field. The electrostatic force applied at the interface is the combination of the charge density of a dielectric at its interface given by (Eq. 4):

$$\sigma = (\varepsilon_{\mathrm{p}} - 1)\varepsilon_0 \mathrm{E} \cdot \hat{\boldsymbol{n}} \tag{4}$$

where **E** and $\hat{\boldsymbol{n}}$are the electric field and unit normal vector at the liquid–air interface, respectively. The electrostatic force is given by (Eq. 5)

$$\boldsymbol{F} = \boldsymbol{E}q \tag{5}$$

Combining these equations gives the force per unit area at the interface as (Eq. 6):

$$\frac{\boldsymbol{F}}{A} = ((\varepsilon_{\mathrm{p}} - 1)\varepsilon_0 \boldsymbol{E} \cdot \hat{\boldsymbol{n}})\boldsymbol{E} \tag{6}$$

Simulation of a two-dimensional periodic microstructure, with 50-μm radius of the feature, 50-μm thickness layer of PDMS, 50-μm between feature and 10-μm air gap, were carried out as shown in Fig. 4. As the spatial heterogeneity of the electrostatic field is induced by the patterned top electrode, the polymer liquid grows upward firstly under the protrusion of the top electrode due to the higher voltage and electric field causing a greater force, depleting the liquid under the cavity (Fig. 4a). The growing polymer touches the protrusive surface of the top electrode and then flows along the inner surface into the cavity because of the capillary action (Fig. 4b, c). The liquid continues to flow upward and converges at the top, achieving self-encapsulation of the hollow microstructure (Fig. 4d).

Figure 5 shows how the voltage and electric field change as the surface moves, as can be seen as the voltage distribution close to the top mask begins to spread out, which, in turn, causes a higher electrostatic force at the interface.

## 5 Experimental results

The manufacture of microstructures has been demonstrated experimentally in polymers as thick as several tens of microns with AC electric fields of frequency ranging from 0 to 1 kHz. Moreover, it has also been shown that the hollow microstructure can always be fabricated independently of the orientation or tilt of the experimental setup. It is observed that the polymer always grows up toward the protrusions of the nickel master electrode under the drive of the electrostatic pressure. This independence of the polymer growth on the orientation of the setup makes this method possible for microfabrication on 3-D surfaces provided that a conformal master is available.

By using the above fabrication method, encapsulated hollow microchannels and microcapsules of different sizes have been fabricated. Figure 6 shows fabricated hollow microchannels of rectangular and round cross sections. The hollow microchannel, shown on the top left picture of Fig. 6, has a width of 100 μm and height of 99 μm. In this

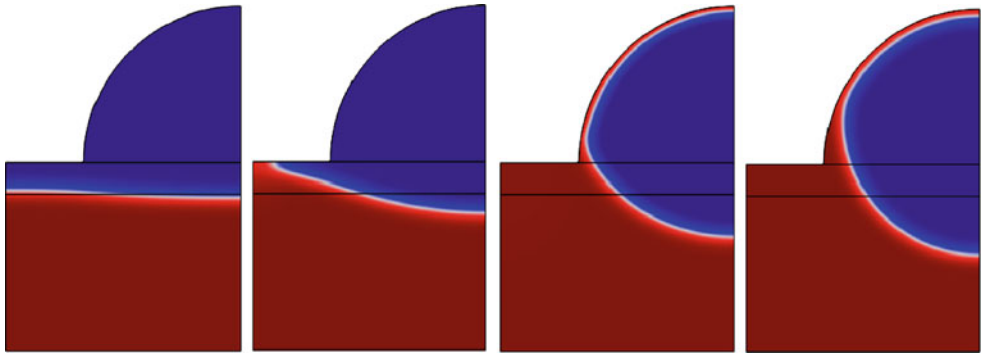


**Fig. 4** Spatio-temporal evolution of a 50 μm-thick polymer liquid interface. *Red* colour represents the polymer liquid and *blue* colour represents air (colour figure online)

**Fig. 5** Evolution of electric fields at various times. Dimensions in μm

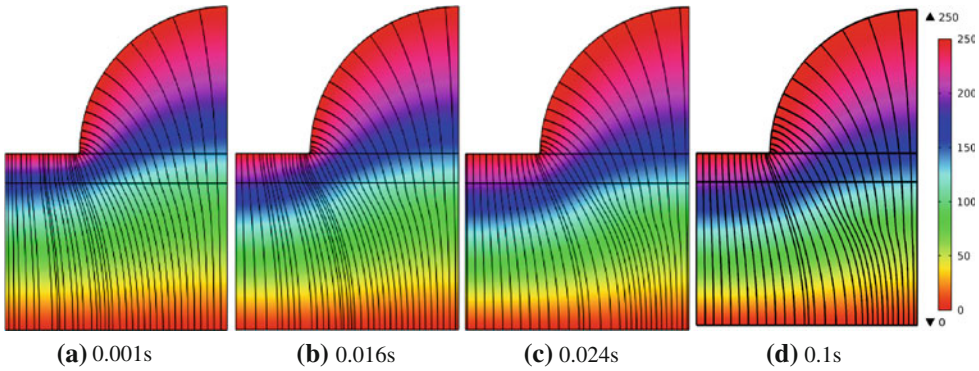


experiment, the initial film thickness of PDMS was 22 μm and the spacer had a thickness of around 100 μm. An AC sinusoidal voltage of 1 kV peak to peak with a frequency of 50 Hz was applied to the master electrode. The thickness of the membrane at the top of the structure is of the order of several microns. Such a thickness permits the conservation of the shape of the high-aspect ratio hollow microchannels even after release from the master. The structures presented in Fig. 6 were manufactured in ambient environment. It is however possible to encapsulate different kind of gases, or even liquids, into the sealed hollow microchannel by performing the fabrication process in a suitable environment. The bottom right picture of Fig. 6 shows the flexibility of the hollow microchannel. The structure retains its shape very well even after bending or delamination from the substrate.

Hollow microcapsules with different shapes have also been manufactured, as shown in Fig. 7. Capsules with a square base (top left picture of Fig. 7) or round base (top right picture of Fig. 7) have been fabricated. The bottom left picture shows the tear of the microcapsule with the shape of a round base, from which one can see clearly that the inside of the microcapsule is hollow. In addition, from the bottom left picture of Fig. 7, the whole inner surface of the microcapsule is actually pretty smooth, which is normally quite difficult to achieve with other microfabrication methods. The bottom right picture of Fig. 7 displays an empty microlens with smooth inner and outer surfaces, allowing thereby the possibility to use the microstructure as a liquid optical microlens. In Fig. 7 all microcapsules are separated from each other. Microcapsules with hollow microchannels have also been connected to construct complex structures, demonstrating the possibility to cascade the manufacturing process. Figure 8 shows the microcapsule array connected with hollow microchannels. The right hand side picture of Fig. 8 shows the inlet or outlet of the hollow microchannel connecting with a reservoir with a diameter of around 350 μm.

## 6 Conclusion

In conclusion, a one-step manufacturing process of encapsulated hollow polymeric microstructures using electric field-assisted capillary action has been successfully developed and demonstrated. Different shapes of hollow microstructures including hollow microchannels and microcapsules have been fabricated in PDMS. The fabricated hollow microstructures have a smooth inner surface. Although PDMS was used in this work, other polymeric

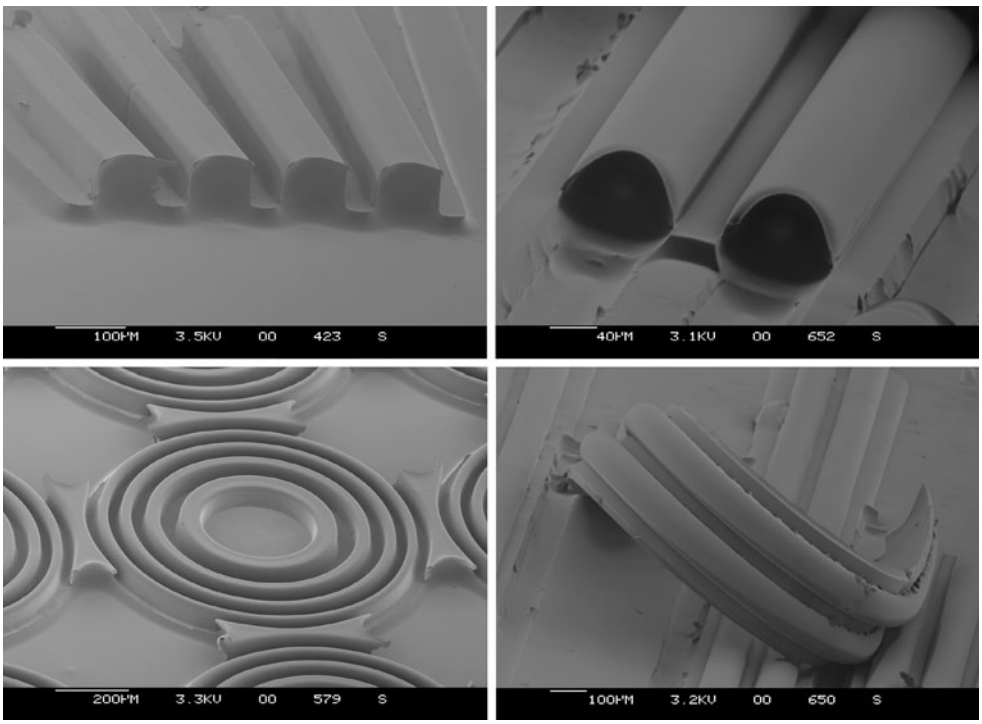


**Fig. 6** Hollow microchannels fabricated in PDMS with different shapes

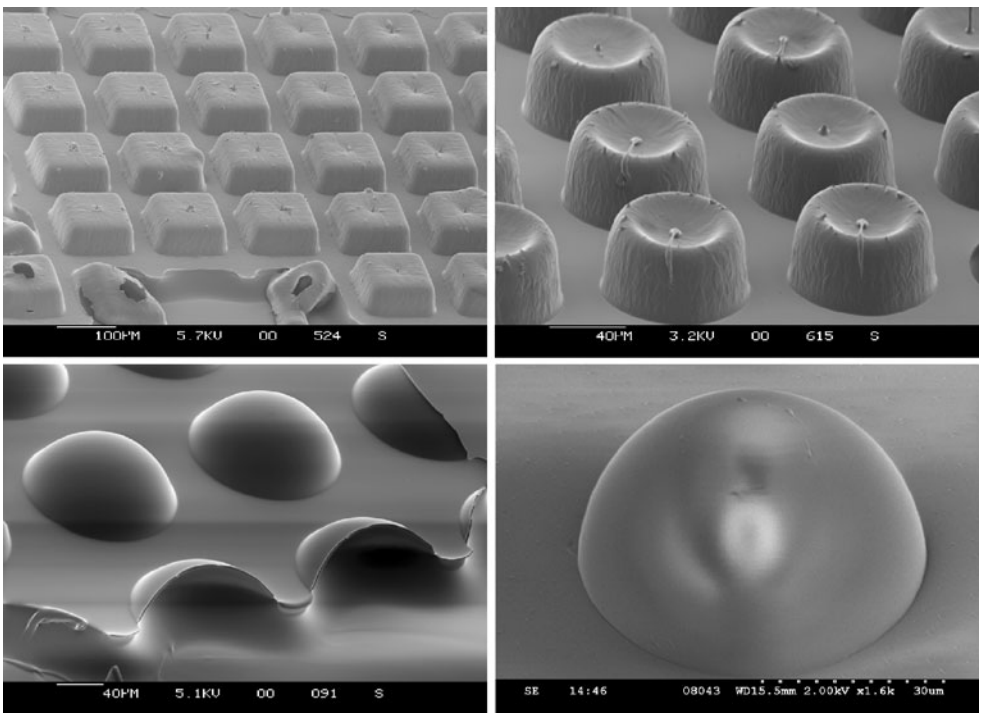


**Fig. 7** Hollow microcapsules with different shapes

materials with similar surface tension properties would also be suitable for this fabrication method. The only drawback of the method presented is that it is only applicable to polymers as opposed to hard materials such as glass, silicon and other materials. To understand the process, a multi-physics model has been developed to study the dynamic process of the (i) the initial movement of PDMS (from a flat surface) to (ii) the formation of the hollow microstructures

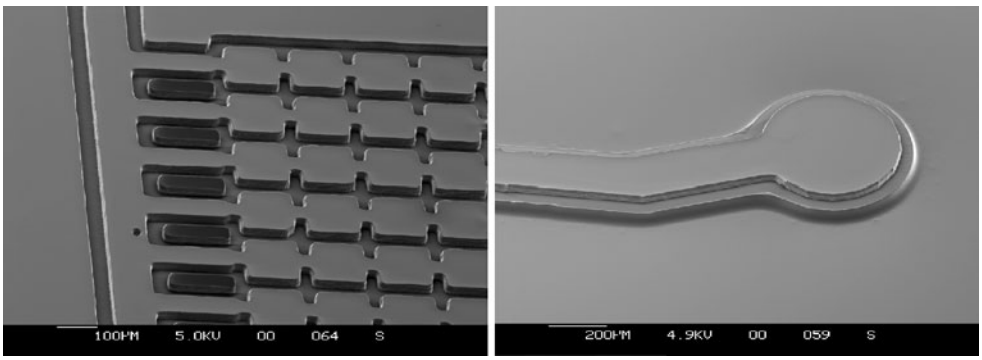


**Fig. 8** Hollow microcapsules connected by hollow microchannels

(once the PDMS has reached the pattern mask). The simulation results concerning the resulting cross sections achievable agree well with those obtained experimentally. Further simulation work is needed to identify the impact on the process by the following parameters: frequency, voltage, mold shape, viscosity, contact angle and the thickness of the polymer liquid. Although only the fabrication of the hollow microstructures has been touched upon and demonstrated in this work, theoretically it should be possible to expand this work to hollow nanostructures. To achieve this, the experimental setup needs to be improved to be able to control accurately the air gap between the master and the polymer at a submicron level.

## References

Atta A, Crawford DG, Koch CR, Bhattacharjee S (2011) Influence of electrostatic and chemical heterogeneity on the electric-field-induced destabilization of thin liquid films. Langmuir 27:12472–12485

Barber JP, Conkey DB, Lee JR, Hubbard NB, Howell LL, Schmidt H, Hawkins AR (2005) Fabrication of hollow waveguides with sacrificial aluminum cores. IEEE Photonics Technol Lett 17: 363–365

Bruinink CM, Peter M, Maury PA, Boer MD, Kuipers L, Huskens J, Reinhoudt DN (2006) Capillary force lithography: fabrication of functional polymer templates as versatile tools for nanolithography. Adv Funct Mater 16:1555–1565

Cai YR, Pan HH, Xu XR, Hu QH, Li L, Tang RK (2007) Ultrasonic controlled morphology transformation of hollow calcium phosphate nanosphere: a smart and biocompatible drug release. Chem Mater 19:3081–3083

Choi J, Lee K-H, Yang S (2011) Fabrication of PDMS through-holes using the MIMIC method and the surface treatment by atmospheric-pressure $CH_4$/He RF plasma. J Micromech Microeng 21:097001–097008

Guijt RM, Baltussen E, van der Steen G, Schasfoort RB, Schlautmann S, Billiet HA, Frank J, van Dedem GW, van den Berg A (2001) New approaches for fabrication of microfluidic capillary electrophoresis devices with on-chip conductivity detection. Electrophoresis 22:235–241

LaFratta CN, Li L, Fourkas JT (2006) Soft-lithographic replication of 3D microstructures with closed loops. PNAS 13:8589–8594

Lin Z, Kerle T, Russell TP, Schaffer E, Steiner U (2002) Electric field induced dewetting at polymer/polymer interfaces. Macromolecules 35:6255–6262

Lippmann MG (1875) Relations entre les phenomenes electrique et capillaires. Ann Chim Phys 5:494–549

Lou X, Archer LA, Yang Z (2008) Hollow Micro/Nanostructures: synthesis and applications. Adv Mater 20:3987–4019

Marariu MD, Voicu NE, Schaffer E, Lin A, Russell TP, Steiner U (2002) Hierarchical structure formation and pattern replication induced by and electric field. Nat Mater 2:48–52

Melin J, Quake SR (2007) Microfluidic large-scale integration: the evolution of design rules for biological automation. Annu Rev Biophys Biomol Struct 36:213–231

Peeni BA, Lee ML, Hawkins AR, Woolley AT (2006) Sacrificial layer microfluidic device fabrication methods. Electrophoresis 27:4888–4895

Salac D, Lu W, Wang C, Sastry AM (2004) Pattern formation in a polymer thin film induced by an in-plane electric field. Appl Phys Lett 85:1161–1163

Schaffer E, Thurn-Albrecht T, Russell TP, Steiner U (2000) Reduction in the surface energy of liquid interfaces at short length scales. Nature 403:871–874

Schaffer E, Thurn-Albrecht T, Russell TP, Steiner U (2001) Electrohydrodynamic instabilities in polymer films. Euro Phys Lett 53:518–524

Sokolova VV, Radtke I, Heumann R, Epple M (2006) Effective transfection of cells with multi-shell calcium phosphate-DNA nanoparticles. Biomaterials 27:3147–3153

Squires TM (2005) Microfluidics: fluid physics at the nanoliter scale. Rev Mod Phys 77:977–1026

Suh KY, Lee HH (2002) Capillary force lithography: large-area patterning, self-organization, and anisotropic dewetting. Adv Funct Mater 12:405–413

Suh KY, Kim YS, Lee HH (2001) Capillary force lithography. Adv Mater 13:1386–1389

Thorsen T, Maerkl SJ, Quake SR (2002) Microfluidic large-scale integration. Science 298:580–584

Unger MA, Chou HP, Thorsen T, Scherer A, Quake SR (2000) Monolithic microfabricated valves and pumps by multilayer soft lithography. Science 288:113–116

Wu N, Russel WB (2009) Micro- and nano-patterns created via electrohydrodynamic instabilities. Nano Today 4:180–192

Xia Y, Whitesides GM (1998) Soft lithography. Annu Rev Mater Sci 28:153–184

Zhu YF, Shi JL, Shen WH, Dong XP, Feng JW, Ruan ML, Li YS (2005) Stimuli-responsive controlled drug release from a hollow mesoporous silica sphere/polyelectrolyte multilayer core–shell structure. Angew Chem Int Ed 44:5083–5087